■ PAPER ■

IMPROVEMENT OF DOSE CALCULATION ACCURACY ON kV CBCT IMAGES WITH CORRECTED ELECTRON DENSITY TO CT NUMBER CURVE

Beom Seok Ahn[*], Hong-Gyun Wu[*,†], Sook Hyun Yoo[*], and Jong Min Park[*]

[*]Department of Radiation Oncology, Seoul National University Hospital

[†]Department of Radiation Oncology, Seoul National University College of Medicine

Received November 21, 2014 / 1st Revised January 16, 2015 / 2nd Revised February 16, 2015 / Accepted for Publication February 17, 2015

To improve accuracy of dose calculation on kilovoltage cone beam computed tomography (kV CBCT) images, a custom-made phantom was fabricated to acquire an accurate CT number to electron density curve by full scatter of cone beam x-ray. To evaluate the dosimetric accuracy, 9 volumetric modulated arc therapy (VMAT) plans for head and neck (HN) cancer and 9 VMAT plans for lung cancer were generated with an anthropomorphic phantom. Both CT and CBCT images of the anthropomorphic phantom were acquired and dose-volumetric parameters on the CT images with CT density curve (CT_{CT}), CBCT images with CT density curve ($CBCT_{CT}$) and CBCT images with CBCT density curve ($CBCT_{CBCT}$) were calculated for each VMAT plan. The differences between CT_{CT} vs. $CBCT_{CT}$ were similar to those between CT_{CT} vs. $CBCT_{CBCT}$ for HN VMAT plans. However, the differences between CT_{CT} vs. $CBCT_{CT}$ were larger than those between CT_{CT} vs. $CBCT_{CBCT}$ for lung VMAT plans. Especially, the differences in $D_{98\%}$ and $D_{95\%}$ of lung target volume were statistically significant (4.7% vs. 0.8% with p = 0.033 for $D_{98\%}$ and 4.8% vs. 0.5% with p = 0.030 for $D_{95\%}$). In order to calculate dose distributions accurately on the CBCT images, CBCT density curve generated with full scatter condition should be used especially for dose calculations in the region of large inhomogeneity.

Keywords : Cone beam computed tomography, Dose calculation, Inhomogeneity correction, Volumetric modulated arc therapy

1. INTRODUCTION

On the strength of image-guided radiation therapy (IGRT), it has been possible to deliver more conformal prescription dose to the target volume, as well as reduce dose to normal tissue, resulting decrease in complications due to radiation therapy [1]. Kilo-voltage cone beam computed tomography (kV CBCT) which is one of IGRT systems, generates 3-dimensional volumetric images of a patient with a single gantry rotation before or after treatment [2]. With this volumetric image set, patient setup can be identified whether it is same as the simulation setup or not, by registering planning computed tomography (CT) image set. Patient setup can be corrected with information acquired by kV CBCT image set, thereby, the intended dose distribution can be delivered accurately [3]. Due to its superiority to the other imaging modalities, kV CBCT has been widely adopted in the clinic despite the increase of imaging dose to a patient [2].

During radiation therapy, deformation or dislocation of organs sometimes occurs during fractionation of radiation therapy, which disturbs an accurate delivery of planned dose to a patient since a patient body is not rigid [4]. The kV CBCT is also a kind of CT image set, therefore, dose distributions can be calculated on

Corresponding author : Jong Min Park, leodavinci@naver.com
101 Daehak-ro, Jongno-gu, Seoul, 110-744

the kV CBCT image set. If we can calculate dose distributions accurately on the CBCT with inhomogeneity corrections, the dosimetric effect caused by the deformation of patient body or slight anatomical changes in locations inside a patient body can be identified and considered during the course of radiation therapy [5-7]. Rong *et al.* generated site-specific CT number to electron density curve with a modification of Computerized Imaging Reference Systems (CIRS^{TM}) density phantom (Computerized Imaging Reference Systems, Inc., Norfolk, VA, USA) and investigated the dosimetric accuracy of the calculated dose distributions on the CBCT image sets [6]. Guan and Dong investigated the dose accuracy calculated on the CBCT with both modified mini CT QC phantom (Fluke Biomedical Corp., Everett, WA, USA) and Catphan^{TM} (The Phantom Laboratory, Salem, NY, USA) in pelvic region [5]. They showed inaccuracy of calculated dose with density curve generated with Catphan^{TM} due to use of Teflon [5].

As recommended by previous study, we made a custom-made phantom which could consider full scatter of kV CBCT during acquisition of CT numbers [5, 6]. The accuracy of dose calculation on the CBCT images with kV CBCT density curve generated using custom-made phantom was compared to that with CT density curve using VMAT plans from the clinical point of view.

2. MATERIALS AND METHODS

2.1 Electron density vs. CT number

The custom-made phantom is shown in Fig.1. For full scatter of CBCT x-ray, additional materials made of acrylic were added along craniocaudal direction. The diameter and the longitudinal length of phantom were 18 cm and 30 cm, respectively. For the insertion of density materials of CIRS^{TM} density phantom, a total of 9 holes were drilled in the central region of the phantom. The density curve with CT simulator (Brilliance CT Big Bore^{TM}, Philips, Cleveland, OH, USA) was acquired using CIRS^{TM} density phantom. During acquisition of density curve for HN region, the values of kVp and mAs were 120 kVp and 300 mAs/slice while those were 120 kVp and 250 mAs/slice for abdomen region. The density curves for CBCT using On-Board Imager^{TM} (OBI, Varian Medical Systems, Palo Alto, CA, USA) were acquired using both a CIRS^{TM} density phantom and a custom-made phantom with same density materials of CIRS^{TM} density phantom. The acquisition parameters were 100 kVp and 145 mAs for HN region and 125 kVp and 680 mAs for abdomen region. Full fan mode was used for the image acquisition with HN protocol while half fan mode was used with abdomen protocol.

2.2 Generation of VMAT plans

Computed tomography images of HN and chest regions of anthropomorphic phantom using planning CT simulator were acquired with same acquisition parameters as used to acquire the density curves. The CBCT image sets of HN and chest regions of the anthropomorphic phantom were also acquired using OBI system. On the CT images, various organs as well as virtual target volumes were contoured for VMAT planning. Nine HN VMAT plans as well as nine lung VMAT plans (a total of 18 VMAT plans) were generated with virtual target volumes. The detailed information of each VMAT plan is shown in Table 1. For the optimization and dose calculation of VMAT

Fig. 1. (a) To consider large geometry of cone beam, a custom-made phantom was fabricated. (b) In the central region of phantom, there were a total of 9 holes for the insertion of density materials from CIRS phantom. Additional acrylic materials were added in the craniocaudal direction to apply full scatter of cone beam computed tomography (CBCT).

Table 1. Volumetric Modulated Arc Therapy Plan Information.

Patient number	Treatment site	Monitor unit (MU)	Prescription dose (Gy)	Fraction number	Arc number	Arc information
1	Head and neck	345	63	35	1	Full
2	Head and neck	320	63	35	2	Partial
3	Head and neck	338	63	35	2	Partial
4	Head and neck	330	63	35	1	Full
5	Head and neck	519	63	35	1	Full
6	Head and neck	317	63	35	2	Partial
7	Head and neck	375	63	35	2	Full
8	Head and neck	390	63	35	2	Partial
9	Head and neck	362	63	35	2	Partial
10	Lung	413	66	33	2	Partial
11	Lung	379	61.2	34	1	Full
12	Lung	436	61.2	34	1	Full
13	Lung	461	66	33	2	Partial
14	Lung	554	45	25	1	Full
15	Lung	338	45	25	2	Full
16	Lung	477	66	33	2	Partial
17	Lung	524	45	15	2	Partial
18	Lung	411	66	33	2	Partial

plans, the progressive resolution optimizer 3 (PRO3, ver.10, Varian Medical Systems, Palo Alto, CA, USA) and the anisotropic analytic algorithm (AAA, ver.10, Varian Medical Systems, Palo Alto, CA, USA) were used. Every VMAT plan was generated using the Eclipse^{TM} system (Varian Medical Systems, Palo Alto, CA, USA). For every VMAT plan, 6 MV photon beams of TrueBeam STx^{TM} (Varian Medical Systems, Palo Alto, CA, USA) with high-definition multi-leaf collimators (MLCs) were used. The calculation grid was 2.5 mm. After generation of VMAT plans using CT images, dose distributions were calculated on the planning CT images as well as CBCT images. Structures contoured on the CT images were also used for the calculation of dose-volumetric parameters on the CBCT images.

2.3 Calculation of dose-volumetric parameters

For both HN and lung VMAT plans, mean, maximum and minimum dose to the target volumes were calculated. The dose received at 95% volume of target volume ($D_{95\%}$), $D_{98\%}$ and the volume irradiated by 95% of prescription dose ($V_{95\%}$) were also calculated for the target volume. For organs at risk (OARs) of HN VMAT plans, maximum dose to spinal cord, mean doses to both parotid glands, both submandibular glands and thyroid glands were calculated. For OARs of lung VMAT plans, maximum doses to spinal cord, ribs, heart and esophagus were calculated. For dose calculations on the CT images, density curve with planning CT simulator was used (CT_{CT}). In the case of dose calculations on the CBCT images, density curve with planning CT simulator ($CBCT_{CT}$) as well as density curve with CBCT ($CBCT_{CBCT}$) was used. In other words, 2 kinds of dose distributions were calculated on the CBCT images with 2 kinds of density curves.

2.4 Data analysis

The dose-volumetric parameters calculated on the CT_{CT} were considered as references in this study. The percent differences in the values of dose-volumetric parameters between $CBCT_{CT}$ and CT_{CT} as well as $CBCT_{CBCT}$ and CT_{CT} were calculated. The percent differences were calculated as follows.

$$Difference\,(\%) = \frac{DV_{CBCT} - DV_{CT}}{DV_{CT}} \times 100 \qquad (1)$$

where, DV_{CBCT} is a value of a dose-volumetric parameter calculated on CBCT images and DV_{CT} is a value of a dose-volumetric parameter calculated on the CT images.

The statistical significances of differences were investigated with paired t-test. Since the differences with positive and negative sign could be cancelled out, the absolute values of differences were acquired and averaged. The statistical significances of those differences in absolute values were also investigated with paired t-test.

3. RESULTS

3.1 Mass density and electron density vs. CT numbers

The electron density vs. CT numbers of planning

Table 2. Dose-volumetric Parameters of Head and Neck VMAT* Plans Calculated at CT_{CT} †, $CBCT_{CT}$ ‡ and $CBCT_{CBCT}$§.

	CT_{CT}	$CBCT_{CT}$	$CBCT_{CBCT}$	Differences between CT_{CT} and $CBCT_{CT}$ (%)	Differences between CT_{CT} and $CBCT_{CBCT}$ (%)
Target volume					
Mean.‖ (Gy)	64.43 ± 0.32	64.76 ± 0.48	64.81 ± 0.43	0.5 ± 0.4 (p = 0.013)	0.6 ± 0.4 (p = 0.002)
Max.¶ (Gy)	68.59 ± 0.75	69.62 ± 1.57	69.49 ± 1.54	1.5 ± 1.8 (p = 0.052)	1.3 ± 1.7 (p = 0.066)
Min.# (Gy)	41.55 ± 11.18	47.91 ± 10.02	48.08 ± 10.13	17.9 ± 11.3 (p = 0.001)	18.2 ± 11.1 (p < 0.001)
$D_{98\%}$** (Gy)	61.74 ± 0.00	61.78 ± 0.65	62.01 ± 0.56	0.1 ± 1.0 (p = 0.876)	0.4 ± 0.9 (p = 0.214)
$D_{95\%}$ (Gy)	62.67 ± 0.15	62.77 ± 0.30	62.93 ± 0.25	0.2 ± 0.6 (p = 0.457)	0.4 ± 0.5 (p = 0.039)
$V_{95\%}$†† (%)	99.0 ± 0.0	99.0 ± 0.0	100.0 ± 0.0	0.0 ± 0.4 (p = 0.954)	1.1 ± 0.3 (p = 0.313)
Organs at risk					
Max. to spinal cord (Gy)	31.70 ± 13.24	31.76 ± 13.36	31.84 ± 13.39	0.1 ± 0.9 (p = 0.615)	1.2 ± 0.9 (p = 0.257)
Mean. to right parotid gland (Gy)	6.23 ± 4.25	7.39 ± 5.16	7.41 ± 5.18	16.4 ± 4.2 (p = 0.007)	16.8 ± 4.4 (p = 0.007)
Mean. to left parotid gland (Gy)	5.64 ± 3.64	6.59 ± 4.36	6.63 ± 4.39	14.7 ± 5.3 (p = 0.006)	15.2 ± 5.7 (p = 0.006)
Mean. to right submandibular gland (Gy)	28.16 ± 14.07	28.54 ± 14.19	28.53 ± 14.20	1.4 ± 1.5 (p = 0.020)	1.3 ± 1.5 (p = 0.025)
Mean. to left submandibular gland (Gy)	27.09 ± 14.31	27.50 ± 14.45	27.50 ± 14.46	1.7 ± 1.3 (p = 0.022)	1.6 ± 1.3 (p = 0.029)
Mean. to thyroid gland (Gy)	12.55 ± 18.32	12.58 ± 18.33	12.54 ± 18.29	0.8 ± 0.6 (p = 0.415)	-0.8 ± 0.8 (p = 0.467)

*VMAT = volumetric modulated arc therapy, †CT_{CT} = computed tomography (CT) images generated with electron density curve acquired with CT, ‡$CBCT_{CT}$ = cone beam computed tomography (CBCT) images calculated with electron density curve acquired with CT, §$CBCT_{CBCT}$ = CBCT images calculated with electron density curve acquired with CBCT, ‖Mean. = mean dose, ¶Max. = maximum dose, #Min. = minimum dose, **$D_{n\%}$ = dose received at n% volume of structure, ††$V_{n\%}$ = volume received by n% of prescription dose.

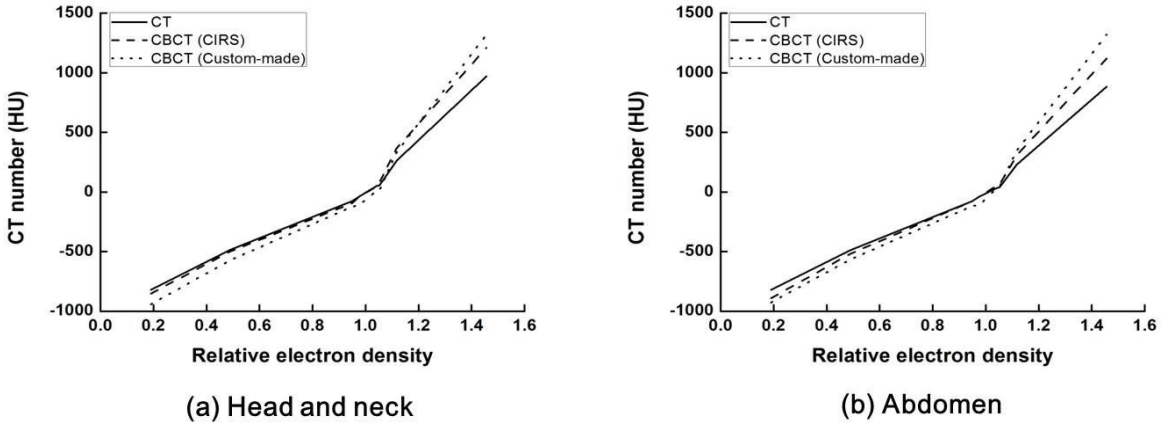

Fig. 2. Relative electron density vs. CT number curve by (a) head and neck image acquisition protocol and (b) abdomen protocol are plotted. Curves acquired with fan beam CT with CIRS phantom, cone beam computed tomography (CBCT) with CIRS phantom and CBCT with custom-made phantom are plotted with solid, dashed and dotted line, respectively.

CT simulator acquired with CIRS™ density phantom as well as those of CBCT with CIRS™ density phantom and custom-made phantom are shown in Fig. 2. Similar to the previous study, considerable differences were observed among density curves [5, 6].

3.2 Changes in dose-volumetric parameters of head and neck VMAT plans

The calculated dose-volumetric parameters of HN VMAT plans on the CT_{CT}, $CBCT_{CT}$ and $CBCT_{CBCT}$ are shown in Table 2. To compare $CBCT_{CT}$ to CT_{CT}, the largest difference was observed at the minimum

Table 3. Percent Differences in Absolute Values of Dose-volumetric Parameters Calculated with $CBCT_{CT}$* vs. Reference and $CBCT_{CBCT}$† vs. Reference for Head and Neck Volumetric Modulated Arc Therapy.

	Target volume					
	Mean.‡	**Max.§**	**Min.‖**	**$D_{98\%}$¶**	**$D_{95\%}$**	**$V_{95\%}$#**
$CBCT_{CT}$ vs. reference	0.5 ± 0.4	*1.7 ± 1.6*	*17.9 ± 11.3*	0.9 ± 0.5	0.5 ± 0.3	0.3 ± 0.2
$CBCT_{CBCT}$ vs. reference	0.6 ± 0.4	*1.5 ± 1.6*	*18.2 ± 11.1*	0.9 ± 0.5	0.5 ± 0.3	0.2 ± 0.2
p	0.218	*0.014*	*0.029*	0.971	0.943	0.278

	Organs at risk					
	Spinal cord Max.	**Right parotid gland Mean.**	**Left parotid gland Mean.**	**Right sub-mandibular gland Mean.**	**Left sub-mandibular gland Mean.**	**Thyroid gland Mean.**
$CBCT_{CT}$ vs. reference	0.8 ± 0.5	*16.4 ± 4.2*	14.7 ± 5.3	1.7 ± 1.1	1.7 ± 1.3	0.9 ± 0.5
$CBCT_{CBCT}$ vs. reference	0.8 ± 0.6	*16.8 ± 4.4*	15.2 ± 5.7	1.7 ± 1.2	1.6 ± 1.3	0.8 ± 0.7
p	0.469	*0.034*	0.069	0.232	0.493	0.946

*$CBCT_{CT}$ = cone beam computed tomography (CBCT) images calculated with electron density curve acquired with computed tomography (CT), †$CBCT_{CBCT}$ = CBCT images calculated with electron density curve acquired with CBCT, ‡Mean. = mean dose, §Max. = maximum dose, ‖Min. = minimum dose, ¶$D_{n\%}$ = dose received at n% volume of structure, #$V_{n\%}$ = volume received by n% of prescription dose.

Table 4. Dose-volumetric Parameters of Lung VMAT* Plans Calculated at CT_{CT} †, $CBCT_{CT}$ ‡ and $CBCT_{CBCT}$§

	CT_{CT}	**$CBCT_{CT}$**	**$CBCT_{CBCT}$**	**Differences between CT_{CT} and $CBCT_{CT}$ (%)**	**Differences between CT_{CT} and $CBCT_{CBCT}$ (%)**
Target volume					
Mean.‖ (Gy)	59.43 ± 9.90	57.84 ± 8.64	59.49 ± 9.90	-2.3 ± 3.6 (p = 0.101)	0.1 ± 0.5 (p = 0.612)
Max.¶ (Gy)	62.54 ± 9.96	60.42 ± 10.73	62.79 ± 10.34	-3.0 ± 10.4 (p = 0.441)	0.3 ± 1.1 (p = 0.343)
Min.# (Gy)	48.93 ± 10.02	48.37 ± 9.34	51.31 ± 11.13	-0.8 ± 4.5 (p = 0.540)	4.6 ± 3.8 (p = 0.011)
$D_{98\%}$** (Gy)	56.77 ± 9.14	54.07 ± 7.21	57.14 ± 9.19	-4.2 ± 4.9 (p = 0.040)	0.6 ± 0.7 (p = 0.039)
$D_{95\%}$ (Gy)	57.61 ± 9.39	54.80 ± 7.38	57.78 ± 9.37	-4.3 ± 5.0 (p = 0.041)	0.3 ± 0.6 (p = 0.219)
$V_{95\%}$†† (%)	100.0 ± 0.0	85.0 ± 24.0	100.0 ± 0.1	-15.0 ± 24.1 (p = 0.117)	0.2 ± 0.1 (p = 0.005)
Organs at risk					
Max. to spinal cord (Gy)	25.73 ± 14.28	25.91 ± 14.30	25.54 ± 14.21	1.0 ± 1.7 (p = 0.252)	-0.7 ± 1.3 (p = 0.221)
Max. to right rib (Gy)	38.18 ± 21.70	33.51 ± 19.63	34.25 ± 20.39	-9.9 ± 13.8 (p = 0.088)	-9.2 ± 12.2 (p = 0.088)
Max. to left rib (Gy)	37.51 ± 21.95	35.85 ± 19.83	36.02 ± 20.27	-2.1 ± 6.2 (p = 0.288)	-2.4 ± 5.6 (p = 0.312)
Max. to heart (Gy)	51.96 ± 19.67	52.22 ± 20.07	51.85 ± 19.92	0.4 ± 1.4 (p = 0.401)	-0.4 ± 1.1 (p = 0.659)
Max. to esophagus (Gy)	32.16 ± 19.90	31.99 ± 19.69	31.70 ± 19.75	-0.2 ± 1.6 (p = 0.552)	-1.6 ± 1.9 (p = 0.215)

*VMAT = volumetric modulated arc therapy, †CT_{CT} = computed tomography (CT) images generated with electron density curve acquired with CT, ‡$CBCT_{CT}$ = cone beam computed tomography (CBCT) images calculated with electron density curve acquired with CT, §$CBCT_{CBCT}$ = CBCT images calculated with electron density curve acquired with CBCT, ‖Mean. = mean dose, ¶Max. = maximum dose, #Min. = minimum dose, **$D_{n\%}$ = dose received at n% volume of structure, ††$V_{n\%}$ = volume received by n% of prescription dose.

dose to target volume, which was 17.9% (p = 0.001). Considerable differences were also observed in the mean dose to both parotid glands, however, those were expressed in percent values. The differences in Gy unit were only 1.2 Gy for right parotid gland and 1.0 Gy for left parotid gland. To compare $CBCT_{CBCT}$ to CT_{CT}, the maximum difference was observed in the minimum dose to target volume, which was 18.2% (p

Table 5. Percent Differences in Absolute Values of Dose-volumetric Parameters Calculated with $CBCT_{CT}$* vs. Reference and $CBCT_{CBCT}$† vs. Reference for Lung Volumetric Modulated Arc Therapy.

	Target volume					
	Mean.‡	**Max.§**	**Min.‖**	**$D_{98\%}$¶**	**$D_{95\%}$**	**$V_{95\%}$#**
$CBCT_{CT}$ vs. reference	2.7 ± 3.2	4.4 ± 9.9	3.6 ± 2.8	*4.7 ± 4.4*	*4.8 ± 4.5*	15.1 ± 24.1
$CBCT_{CBCT}$ vs. reference	0.4 ± 0.4	0.9 ± 0.7	4.6 ± 3.7	*0.8 ± 0.5*	*0.5 ± 0.4*	0.2 ± 0.1
p	0.074	0.350	0.482	*0.033*	*0.030*	0.118
	Organs at risk					
	Spinal cord Max	**Right rib Max**	**Left rib Max**	**Heart Max**	**Esophagus Max**	
$CBCT_{CT}$ vs. reference	1.3 ± 1.4	10.9 ± 13.0	3.0 ± 5.8	1.4 ± 0.5	0.8 ± 1.4	
$CBCT_{CBCT}$ vs. reference	1.1 ± 1.0	9.7 ± 11.8	2.5 ± 5.6	1.0 ± 0.6	1.7 ± 1.8	
p	0.827	0.278	0.117	0.393	0.065	

*$CBCT_{CT}$ = cone beam computed tomography (CBCT) images calculated with electron density curve acquired with computed tomography (CT), †$CBCT_{CBCT}$ = CBCT images calculated with electron density curve acquired with CBCT, ‡Mean. = mean dose, §Max. = maximum dose, ‖Min. = minimum dose, ¶$D_{n\%}$ = dose received at n% volume of structure, #$V_{n\%}$ = volume received by n% of prescription dose.

< 0.001).

The average absolute values of differences in dose-volumetric parameters of HN VMAT plans between CT_{CT} vs. $CBCT_{CT}$ as well as CT_{CT} vs. $CBCT_{CBCT}$ are shown in Table 3. Every difference between dosimetric errors with $CBCT_{CT}$ and those with $CBCT_{CBCT}$ was less than 1% showing minimal differences. In other words, the accuracy of dose calculation on the $CBCT_{CT}$ was not much different from that on the $CBCT_{CBCT}$ for HN VMAT.

3.3 Changes in dose-volumetric parameters of lung VMAT plans

The calculated dose-volumetric parameters of lung VMAT plans on the CT_{CT}, $CBCT_{CT}$ and $CBCT_{CBCT}$ are shown in Table 4. To compare $CBCT_{CT}$ to CT_{CT}, the largest difference was observed in $V_{95\%}$ of target volume, which was 15%, however, that difference was not statistically significant (p = 0.117). The difference in $D_{98\%}$ and $D_{95\%}$ of target volume were -4.2% and -4.3%, respectively. To compare $CBCT_{CBCT}$ to CT_{CT}, the maximum difference was observed in the maximum dose to right rib, however, that difference was not statistically significant (p = 0.088).

The average absolute values of differences in dose-volumetric parameters of lung VMAT plans between CT_{CT} vs. $CBCT_{CT}$ as well as CT_{CT} vs. $CBCT_{CBCT}$ are shown in Table 5. Except the minimum dose to target volume and maximum dose to esophagus, every difference of CT_{CT} vs. $CBCT_{CBCT}$ was smaller than those of CT_{CT} curve vs. $CBCT_{CT}$. The exceptional cases of the minimum dose to target volume and the maximum dose to esophagus were not statistically significant (p = 0.482 and 0.065, respectively). The magnitudes of differences in lung VMAT plans were larger than those in HN VMAT plans. The dosimetric errors of dose calculation with $CBCT_{CT}$ were reduced by using $CBCT_{CBCT}$. Those were reduced especially in $D_{98\%}$ and $D_{95\%}$ of lung target volume (4.7% vs. 0.8% with p = 0.033 for $D_{98\%}$ and 4.8% vs. 0.5% with p = 0.030 for $D_{95\%}$).

4. DISCUSSION

In this study, no considerable clinically relevant dosimetric differences were observed in VMAT plans for HN cancer while some considerable differences with statistical significances were observed in VMAT plans for lung cancer.

Since the differences in CT numbers of lung and dense bone materials were large as shown in Fig. 2, it was expected large discrepancies in dose would be observed in the regions of very low or very high density tissue. Consequently, large differences were observed in lung VMAT plans which were calculated in the region of large inhomogeneity while small differences were observed in HN VMAT plans calculated in the region of relatively small inhomogeneity. The values of $D_{98\%}$ and $D_{95\%}$ of lung target volume in the $CBCT_{CT}$ were lower than the reference values which were calculated on the CT_{CT}. Therefore, a potential risk to underestimate the delivered dose to lung target volume exists when calculating dose distributions on the $CBCT_{CT}$. Furthermore, the difference in dose-volumetric parameters between CT_{CT} and $CBCT_{CBCT}$ were smaller than those between CT_{CT} and $CBCT_{CT}$. The differences between CT_{CT} vs. $CBCT_{CBCT}$ and CT_{CT} vs. $CBCT_{CT}$ were not statistically significant (p > 0.05) except $D_{98\%}$ and $D_{95\%}$, however, this might be due to

the small sample size to acquire reliable *p* values in this study (9 cases). By utilizing a large sample size, further analysis is needed and this will be done as a future work.

As recommended by previous studies, we made a phantom to apply full scatter of x-ray of CBCT in order to acquire an accurate relationship between CT number and electron density [5, 6]. Although the accuracy in dose calculation was improved, differences between the values of dose-volumetric parameters calculated on CT images and CBCT images still existed. This uncertainty in dose was due to the poor image quality of CBCT [8]. Although evaluations of dose distributions without this uncertainty are not possible when using CBCT images, the discrepancy in dose between CT and CBCT could be reduced by using full scatter density phantom during acquisition of CT number to electron density curve, especially for sites with large inhomogeneity such as chest region.

In this study, we analyzed dose-volumetric parameters calculated with the AAA. The results could be different by using different dose calculation algorithm such as Acuros XB (Varian Medical Systems, Palo Alto, CA, USA). In addition, we used only 6 MV photon beam. An analysis with various energies of photon beams is needed. Further analysis with various dose calculation algorithms as well as various photon beam energies will be done as a future work.

Several studies investigated the changes in the clinically relevant dose-volumetric parameters when calculating on the CBCT images for VMAT technique [8-10]. Most of those studies acquired CBCT density curves using Catphan^{TM} or used same density curve as CT density curve. However, it has been demonstrated that the use of Chaphan^{TM} for dose calculation was not accurate due to Teflon [5]. Rong *et al.* modified CIRS^{TM} density phantom by adding solid water phantom along craniocaudal direction to consider large cone beam geometry of CBCT [6]. Instead of adding solid water phantom, we used a custom-made phantom to generate density curve for CBCT. As shown in the results, the accuracy of dose calculation with density curve using that phantom was better than that with density curve of CT.

5. Conclusion

For accurate calculation of dose distributions on the CBCT images, a density curve for CBCT should be acquired with a density phantom possible to apply full scatter of x-ray of CBCT. From the clinical point of view, the differences in dose distributions in the region of low inhomogeneity with $CBCT_{CT}$ were not large compared to those with $CBCT_{CBCT}$. However, those differences were large in the region of high inhomogeneity such as lung. For an accurate dose calculation on the CBCT images, CBCT density curve with full scatter condition should be used.

REFERENCES

1. Maund IF, Benson RJ, Fairfoul J, Cook J, Huddart R, Poynter A. Image Guided Radiotherapy of the Prostate using Daily Cone Beam CT - The Feasibility and Likely Benefit of Implementing a Margin Reduction. Brit J Radiol. 2014; **87**:20140459.
2. Ding GX, Duggan DM, Coffey CW. Characteristics of kilovoltage x-ray beams used for cone-beam computed tomography in radiation therapy. Phys Med Biol. 2007; **52**(6):1595- 615.
3. Yan D, Ziaja E, Jaffray D, Wong J, Brabbins D, Vicini F, Martinez A. The use of adaptive radiation therapy to reduce setup error: a prospective clinical study. Int J Radiat Oncol. 1998;**41**(3):715-20.
4. Veiga C, McClelland J, Moinuddin S, Lourenco A, Ricketts K, Annkah J, Modat M, Ourselin S, D'Souza D, Royle G. Toward adaptive radiotherapy for head and neck patients: Feasibility study on using CT-to-CBCT deformable registration for "dose of the day" calculations. Med Phys. 2014;**41**(3):031703.
5. Guan H, Dong H. Dose calculation accuracy using cone-beam CT (CBCT) for pelvic adaptive radiotherapy. Phys Med Biol. 2009;**54**(20):6239-50.
6. Rong Y, Smilowitz J, Tewatia D, Tome WA, Paliwal B. Dose calculation on kV cone beam CT images: an investigation of the Hu-density conversion stability and dose accuracy using the site-specific calibration. Med Dosim. 2010;**35**(3): 195-207.
7. Yang Y, Schreibmann E, Li T, Wang C and Xing L, *Evaluation of on-board kV cone beam CT (CBCT)-based dose calculation.* Phys Med Biol, 2007. **52**(3): p. 685-705.
8. Qian J, Lee L, Liu W, Chu K, Mok E, Luxton G, Le QT, Xing L. Dose reconstruction for volumetric modulated arc therapy (VMAT) using cone-beam CT and dynamic log files. Phys Med Biol. 2010;**55**(13):3597-610.
9. Reggiori G, Mancosu P, Tozzi A, Cantone MC, Castiglioni S, Lattuada P, Lobefalo F, Cozzi L,

Fogliata A, Navarria P, Scorsetti M. Cone beam CT pre- and post-daily treatment for assessing geometrical and dosimetric intrafraction variability during radiotherapy of prostate cancer. J Appl Clin Med Phys. 2011;**12**(1):141-152.

10. Jin X, Hu W, Shang H, Han C, Yi J, Zhou Y, Xie C. CBCT-based volumetric and dosimetric variation evaluation of volumetric modulated arc radiotherapy in the treatment of nasopharyngeal cancer patients. Radiat Oncol. 2013;**8**:279.